

# Pigment epithelium-derived factor inhibits proliferation, invasion and angiogenesis, and induces ferroptosis of extravillous trophoblasts by targeting Wnt- $\beta$ -catenin/VEGF signaling in placenta accreta spectrum

RUI LI<sup>1</sup>, XIAOYING WENG<sup>1</sup>, XUYANG HU<sup>1</sup>, JUNJUN WANG<sup>2</sup> and LIN ZHENG<sup>1</sup>

Departments of <sup>1</sup>Obstetrics and Gynecology and <sup>2</sup>Clinical Laboratory, Shengli Clinical Medical College of Fujian Medical University, Fuzhou, Fujian 350028, P.R. China

Received April 17, 2023; Accepted December 29, 2023

DOI: 10.3892/mmr.2024.13199

**Abstract.** Placenta accreta spectrum (PAS) is one of the most dangerous complications in obstetrics, which can lead to severe postpartum bleeding and shock, and even necessitate uterine removal. The abnormal migration and invasion of extravillous trophoblast cells (EVTs) and enhanced neovascularization occurring in an uncontrolled manner in time and space are closely related to the abnormal expression of pro-angiogenic and anti-angiogenic factors. The pigment epithelium-derived factor (PEDF) is a multifunctional regulatory factor that participates in several important biological processes and is recognized as the most efficient inhibitor of angiogenesis. The present study aimed to explore the effects of PEDF on EVT phenotypes and the underlying mechanisms in PAS. HTR-8/SVneo cells were transfected to overexpress or knock down PEDF. Cell proliferation and invasion were assessed using Cell Counting Kit-8, 5-ethynyl-2'-deoxyuridine and Transwell assays. *In vitro* angiogenesis was analyzed using tube formation assays. The degree of ferroptosis was assessed by evaluating the levels of lipid reactive oxygen species, total iron, Fe<sup>2+</sup>, malondialdehyde and reduced glutathione using commercial kits. The expression levels of biomarkers of ferroptosis, angiogenesis, cell proliferation and Wnt signaling were examined by western blotting. PEDF overexpression decreased the proliferation, invasion and angiogenesis, and induced ferroptosis of EVT. Activation of Wnt signaling with BML-284 and overexpression of vascular endothelial growth factor (VEGF) reversed the PEDF overexpression-induced suppression of cell proliferation, invasion and tube formation. PEDF overexpression-induced ferroptosis was

also decreased by Wnt agonist treatment and VEGF overexpression. It was predicted that PEDF suppressed the proliferation, invasion and angiogenesis, and increased ferroptosis in EVT by decreasing Wnt- $\beta$ -catenin/VEGF signaling. The findings of the present study suggested a novel regulatory mechanism of the phenotypes of EVT and PAS.

## Introduction

Extravillous trophoblast cells (EVTs) are a group of cells that serve a critical role in reproduction and development, and are associated with obstetrical and gynecological diseases, such as placenta accreta spectrum (PAS) (1). The migration of placental EVT into the uterine decidua facilitates the establishment of blood circulation between mother and fetus at the early stage of pregnancy and is modulated by EVT-decidual cell interaction (2). It has been demonstrated that excessive migration and invasion of EVT is closely associated with the incidence of PAS (3). Over the past few decades, the incidence of PAS has not decreased despite research efforts (4). Abnormal invasion of EVT and vascular generation are pivotal factors that induce PAS (4). Therefore, further research on EVT is vital for developing preventative measures and therapies for PAS.

The invasion and vascular remodeling of EVT are complex (5). The epidermal growth factor, fibroblast growth factor (FGF), TGF- $\beta$ , Wnt and NOTCH pathways serve crucial roles in placental and development of trophoblasts (6,7). Furthermore, vascular endothelial growth factor (VEGF) and platelet-derived growth factor (PDGF) are closely associated with the process of vascular remodeling, and thus, also participate in the regulation of EVT and PAS (8,9). The pigment epithelium-derived factor (PEDF) is a multifunctional regulatory factor that participates in several important biological processes, including differentiation, inflammation and angiogenesis (10,11). It has previously been demonstrated that upregulated levels of PEDF are involved in cancer progression (12,13). Furthermore, PEDF has been reported to be highly expressed in the vasculature of healthy pregnant patients and placenta trophoblasts, which indicates its role during placental blood vessel formation (14). Nevertheless, the specific role and regulatory mechanisms of PEDF in PAS development are still unclear.

---

*Correspondence to:* Professor Lin Zheng, Department of Obstetrics and Gynecology, Shengli Clinical Medical College of Fujian Medical University, 516 Jinrong South Road, Cangshan, Fuzhou, Fujian 350028, P.R. China  
E-mail: 2924382805@qq.com

**Key words:** extravillous trophoblasts, invasion, angiogenesis, ferroptosis, Wnt,  $\beta$ -catenin, vascular epidermal growth factor

Ferroptosis is a newly identified form of regulated cell death that has drawn great attention in recent years (15). Ferroptosis is characterized by iron-dependent lipid peroxidation and is implicated in the regulation of various diseases, including neurodegenerative diseases, cardiovascular diseases, carcinogenesis and reproductive diseases (16–18). Several factors, especially glutathione peroxidase 4 (GPX4) and solute carrier family 7 member 11 (SLC7A11), have been identified as suppressors of ferroptosis via regulation of the transportation of cysteine and clearance of lipid peroxides (19).

The present study assessed the effects of PEDF on EVT<sub>s</sub> in PAS and explored the potential molecular mechanism.

## Materials and methods

**Cell lines.** The extravillous trophoblast cell line HTR-8/SVneo was purchased from the American Type Culture Collection and maintained in RPMI-1640 medium (HyClone; Cytiva) containing 10% FBS (Gibco; Thermo Fisher Scientific, Inc.), 100 U/ml penicillin and 100 µg/ml streptomycin. All cells were cultured in a 37°C incubator with 5% CO<sub>2</sub>. For BML-284 treatment, the cells were treated with 10 nM BML-284 (HY-19987; MedChemExpress) for 24 h after overexpression treatment for 48 h in a 37°C incubator with 5% CO<sub>2</sub>. For ferrostatin-1 (Fer-1) treatment, cells were incubated with 1 µM ferrostatin-1 (HY-100579; MedChemExpress) for 24 h after overexpression treatment for 48 h in a 37°C incubator with 5% CO<sub>2</sub>.

**Cell transfection.** The PEDF overexpression vector (OE-PEDF; 2 µg; pcDNA3.1+), VEGF overexpression vector (OE-VEGF; 2 µg), empty vector (pcDNA3.1+; 2 µg), small interfering RNA targeting PEDF (siPEDF; 100 nM; sense, 5'-GGAUUUCUA CUUGGAUGAA-3' and antisense, 5'-UUCAUCCAAGUA GAAAUCC-3') and small interfering RNA negative control (siNC; 100 nM; sense, 5'-CUAACUAUCUCGAACGCAAdT dT-3' and antisense, 5'-UUGCGUUCGAGAUAGUUAGdT dT-3') were synthesized by Shanghai GenePharma Co., Ltd. Cell transfection was performed using Lipofectamine® 2000 (Invitrogen; Thermo Fisher Scientific, Inc.) according to the manufacturer's protocol at 37°C for 48 h. PEDF overexpression vectors were mixed with Lipofectamine 2000 reagent alone in DMEM for 20 min or together with the VEGF overexpression vectors. After 48 h, the transfected cells were further processed for the following experiments.

**Cell proliferation.** Cell viability was assessed using a Cell Counting Kit-8 (CCK-8; Beyotime Institute of Biotechnology) and a 5-ethynyl-2'-deoxyuridine (EdU) assay kit (Beyotime Institute of Biotechnology). For the CCK-8 assay, transfected cells were seeded into a 96-well plate at a density of 5,000 cells/well. After incubation in a 37°C incubator for 24 h, CCK-8 reagent was added into each well and the cells were incubated for another 2 h at 37°C. The absorbance values were then measured at 450 nm. For EdU assays, cells were seeded into 96-well plates (5 × 10<sup>3</sup> cells/well) and incubated for 24 h at 37°C, then fixed in 4% paraformaldehyde at room temperature for 30 min and stained with EdU reagent for 2 h at 37°C, followed by DAPI staining at room temperature for 20 min. Images were captured under a fluorescence microscope (Leica Microsystems GmbH).

**Transwell assay.** Transwell plate chambers (8 µm pore size) were coated with Matrigel (BD Biosciences) at 37°C for 30 min before use. For cell migration assays, cells (1 × 10<sup>4</sup>) were suspended in RPMI-1640 medium without FBS and seeded into the upper chamber with no Matrigel, while complete culture medium (RPMI-1640 medium with 10% FBS) was added to the lower chamber. After incubation for 24 h at 37°C, the cells were collected and stained with 0.2% crystal violet in methanol for 10 min at room temperature. The cell invasion was analyzed using the same method, and the cells were added into upper chambers precoated with Matrigel. Five random images were captured under a light microscope (Leica Microsystems GmbH).

**Wound healing assay.** The wound healing assay was conducted to evaluate the migration of cells. The cell monolayer (70–80% confluence as a monolayer) in a 6-well plate was scratched with a 200-µl sterile pipette tip, then washed with PBS and cultured with RPMI-1640 medium (HyClone; Cytiva) containing 0.1% FBS for 12 h. Images of the width of the wound were captured at 0, 6 and 12 h after scratching using a light microscope (Nikon Corporation). The width of wounds was measured using ImageJ software (version 1.54; National Institutes of Health).

**Colony formation assay.** For colony formation assays, HTR-8/SVneo cells were seeded into 6-well plates at a density of 1,000 cells/well. Cells were incubated in a 37°C cell incubator for 14 days. Following fixation with 4% paraformaldehyde at room temperature for 30 min, the colonies were stained with 0.1% crystal violet (MilliporeSigma) at room temperature for 30 min and images were captured and counted under a light microscope (Leica Microsystems GmbH). A cluster with >50 cells was considered a colony. The number of colonies was quantified using ImageJ software (Fiji Version, National Institutes of Health).

**Tube formation assay.** HTR-8/SVneo cells in RPMI-1640 medium with 10% FBS (HyClone; Cytiva) were seeded into a 96-well plate (2 × 10<sup>4</sup> cells/well) pre-coated with Matrigel (Corning, Inc.) at 37°C for 30 min. Following incubation for 8 h at 37°C with 5% CO<sub>2</sub>, the images of formed tubes were captured using a light microscope (Leica Microsystems GmbH).

**Detection of ferroptosis.** To analyze ferroptosis, the levels of lipid reactive oxygen species (ROS), total and ferrous iron (Fe<sup>2+</sup>), malondialdehyde (MDA) and glutathione (GSH) in HTR-8/SVneo cells were examined using a Fluorometric Intracellular ROS Kit (cat. no. MAK143; MilliporeSigma), Iron Assay Kit (cat. no. ab83366; Abcam), Lipid Peroxidation (MDA) Assay Kit (cat. no. MAK085; MilliporeSigma), and GSH and Oxidized Glutathione Assay Kit (cat. no. S0053; Beyotime Institute of Biotechnology), respectively, according to the manufacturers' protocols.

**Reverse transcription-quantitative PCR (RT-qPCR).** Total RNA was extracted from cells and tissues using TRIzol® (Invitrogen; Thermo Fisher Scientific, Inc.), and was purified and reverse transcribed into cDNA with the PrimeScript™ RT

reagent kit (cat. no. RR037A; Takara Biotechnology Co., Ltd.) according to the manufacturer's protocol. The gene expression was determined using a qPCR assay with a SYBR Green mixture kit (Takara Bio, Inc.) according to the manufacturer's instructions. The following thermocycling conditions were used: 94°C for 60 sec, and 40 cycles of 94°C for 5 sec, 60°C for 34 sec and 72°C for 30 sec. mRNA expression levels were quantified using the  $2^{-\Delta\Delta C_q}$  method and normalized to the internal reference gene GAPDH (20). The primer sequence used were: PEDF forward, 5'-CAGAAGAACCTCAAGAGTGCC-3' and reverse, 5'-CTTCATCCAAGTAGAATCC-3'; VEGF forward, 5'-CAACTTCTGGGCTCTTCTCG-3' and reverse, 5'-CCTCTCTCTTCTTCTCTTCC-3'; and GAPDH forward, 5'-CAAGGTCATCCATGACAACCTTG-3' and reverse, 5'-GTCCACCACCCTGTTGCTGTAG-3'.

**Western blotting.** Total protein was extracted from cells or tissues using RIPA lysis buffer (Beyotime Institute of Biotechnology) and quantified using a BCA kit. Protein (35  $\mu$ g per lane) was separated by 12% SDS-PAGE and transferred to PVDF membranes, which were blocked in 5% non-fat milk for 1 h at room temperature. The membranes were then incubated with primary antibodies against GPX4 (1:1,000; ab41787; Abcam), SLC7A11 (1:1,000; ab307601; Abcam), VEGF (1:1,000; cat. no. AF-293-SP; R&D Systems, Inc.), Wnt (1:1,000; ab15251; Abcam),  $\beta$ -catenin (1:1,000; ab32572; Abcam), E-cadherin (1:1,000; ab231303; Abcam), vimentin (1:1,000; ab92547; Abcam), FGF (1:1,000; ab131162; Abcam), PDGF (1:1,000; ab178409; Abcam), proliferating cell nuclear antigen (PCNA; 1:1,000; ab29; Abcam) and  $\beta$ -actin (1:1,000; ab8226; Abcam) for 12 h at 4°C.  $\beta$ -actin was used as the loading control. Membranes were then incubated with goat anti-mouse, goat anti-rabbit or rabbit anti-goat (1:3,000; cat. nos. sc-2005, sc-2004 and sc-2768, respectively; Santa Cruz Biotechnology, Inc.) IgG peroxidase-conjugated secondary antibodies at 37°C for 1 h. Bands were visualized with ECL reagent (Merck KGaA) and semi-quantified using ImageJ software (version 1.47; National Institutes of Health).

**Clinical sample detection.** Placentas from pregnant women who delivered by cesarean section were collected at Shengli Clinical Medical College of Fujian Medical University (Fuzhou, China) between May 2017 and July 2022, including 20 cases in the PAS group (age range, 26-39 years; mean age, 33 years old) and 20 pregnant woman giving birth during a healthy term pregnancy in the healthy group (age range, 20-33 years; mean, 27 years old). The exclusion criteria were as follows: i) Gestational hypertension, diabetes, kidney disease, immune system diseases (including systemic red Lupus maculatus and antiphospholipid syndrome), heart disease, tumor, epilepsy, acute and chronic infectious diseases; ii) deformed or stillborn; and iii) alcohol and addiction to drugs. The diagnostic criteria for placental implantation were as follows: The villi of the placenta invaded the myometrium in varying degrees. MRI examination showed that the base of the lower segment of the uterus was thinning or disappearing, and the boundary between the placenta and the myometrium was unclear, and the placenta even penetrated the myometrium. Intraoperatively, it was confirmed that

placental villi directly invaded the uterine myometrium, as observed on the placental bed in the implanted placenta or the resected uterine specimen.

The tissues were immediately frozen in liquid nitrogen and stored at -80°C for subsequent experiments. The mRNA expression levels of PEDF in these tissues were examined by RT-qPCR. All experiments using clinical samples were approved by the Ethics Committee of Shengli Clinical Medical College of Fujian Medical University (approval no. K2020-090040; Fuzhou, China) in July 2020. All patients provided written informed consent.

**Statistical analysis.** The data are presented as the mean  $\pm$  standard deviation and were analyzed by SPSS 20.0 software (IBM Corp.). All experiments were repeated at least three times. Data with a normal distribution were compared by Student's unpaired t-test. One-way ANOVA followed by Tukey's post hoc test was used to assess the differences among multiple groups.  $P < 0.05$  was considered to indicate a statistically significant difference.

## Results

**PEDF inhibits the proliferation, migration and angiogenesis of EVTs in vitro.** To determine the role of PEDF in PAS, its mRNA expression levels in healthy placentas and placentas from patients with PAS were analyzed. The results of RT-qPCR revealed significantly decreased relative mRNA expression levels of PEDF in the PAS group compared with that in the healthy group, suggesting the potential regulatory effects of PEDF on PAS (Fig. S1). Next, the effects of PEDF on the phenotypes of EVTs were determined using knockdown or overexpression of PEDF. The transfection efficiencies of OE-PEDF, OE-VEGF and siPEDF were confirmed by western blotting. OE-PEDF and OE-VEGF significantly increased relative PEDF and VEGF expression levels compared with the empty vector control. siPEDF significantly decreased the relative expression levels of PEDF compared with those in the siNC group (Fig. S2).

PEDF overexpression significantly decreased the viability (Fig. 1A) and colony formation of EVTs (Fig. 1C) and decreased the number of EdU-positive cells (Fig. 1B) compared with the OE-NC group, whereas PEDF knockdown using siPEDF significantly increased cell proliferation (Fig. 1A) and colony number (Fig. 1C) and increased the number of EdU-positive cells compared with the siNC group.

The Transwell assay indicated a significantly increased number of invasive cells following PEDF knockdown and a significantly decreased number of invasive cells following PEDF overexpression compared with the siNC group and OE-NC group, respectively (Fig. 1D). The wound healing ability of PEDF knockdown cells was higher than that of the siNC group, whereas overexpression of PEDF reduced the wound healing ability (Figs. 1E and S3).

Furthermore, the protein expression levels of the epithelial biomarker E-cadherin were decreased, and the levels of mesenchymal biomarker vimentin, growth factors FGF, VEGF and PDGF, and proliferative biomarker PCNA were elevated by PEDF knockdown, whereas PEDF overexpression had the opposite effect (Fig. 1F).

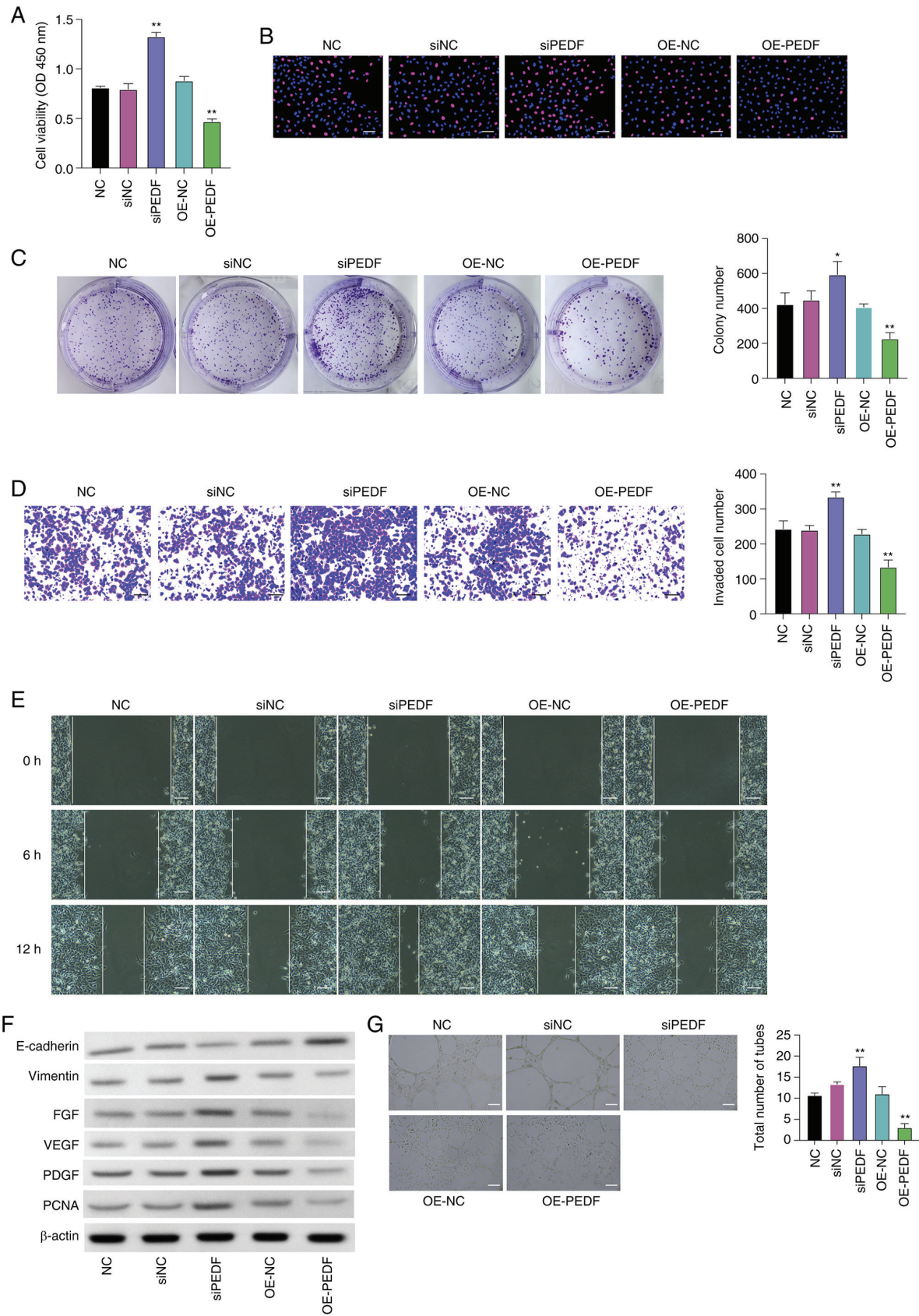


Figure 1. PEDF inhibits the proliferation, migration and angiogenesis of EVT cells *in vitro*. EVT cells were transfected with OE-PEDF or siPEDF. Cell viability and proliferation were assessed using (A) Cell Counting Kit-8, (B) 5-ethynyl-2'-deoxyuridine (red, proliferative cells; blue, nuclei) and (C) colony formation assays. (D) Cell invasion was assessed using a Transwell assay. (E) Cell migration was detected using a wound healing assay. (F) Protein expression levels of E-cadherin, vimentin, FGF, VEGF, PDGF and PCNA were examined by western blotting. (G) *In vitro* angiogenesis was examined using a tube formation assay. Scale bar, 50  $\mu$ m. Data are presented as the mean  $\pm$  SD, n=3. \*P<0.05, \*\*P<0.01 vs. NC or siPEDF. EVT, extravillous trophoblast cell; FGF, fibroblast growth factor; NC, negative control; OD, optical density; OE-NC, control empty vector for overexpression; OE-PEDF, PEDF overexpression vector; PCNA, proliferating cell nuclear antigen; PDGF, platelet-derived growth factor; PEDF, pigment epithelium-derived factor; siNC, small interfering RNA negative control; siPEDF, small interfering RNA targeting PEDF; VEGF, vascular endothelial growth factor.

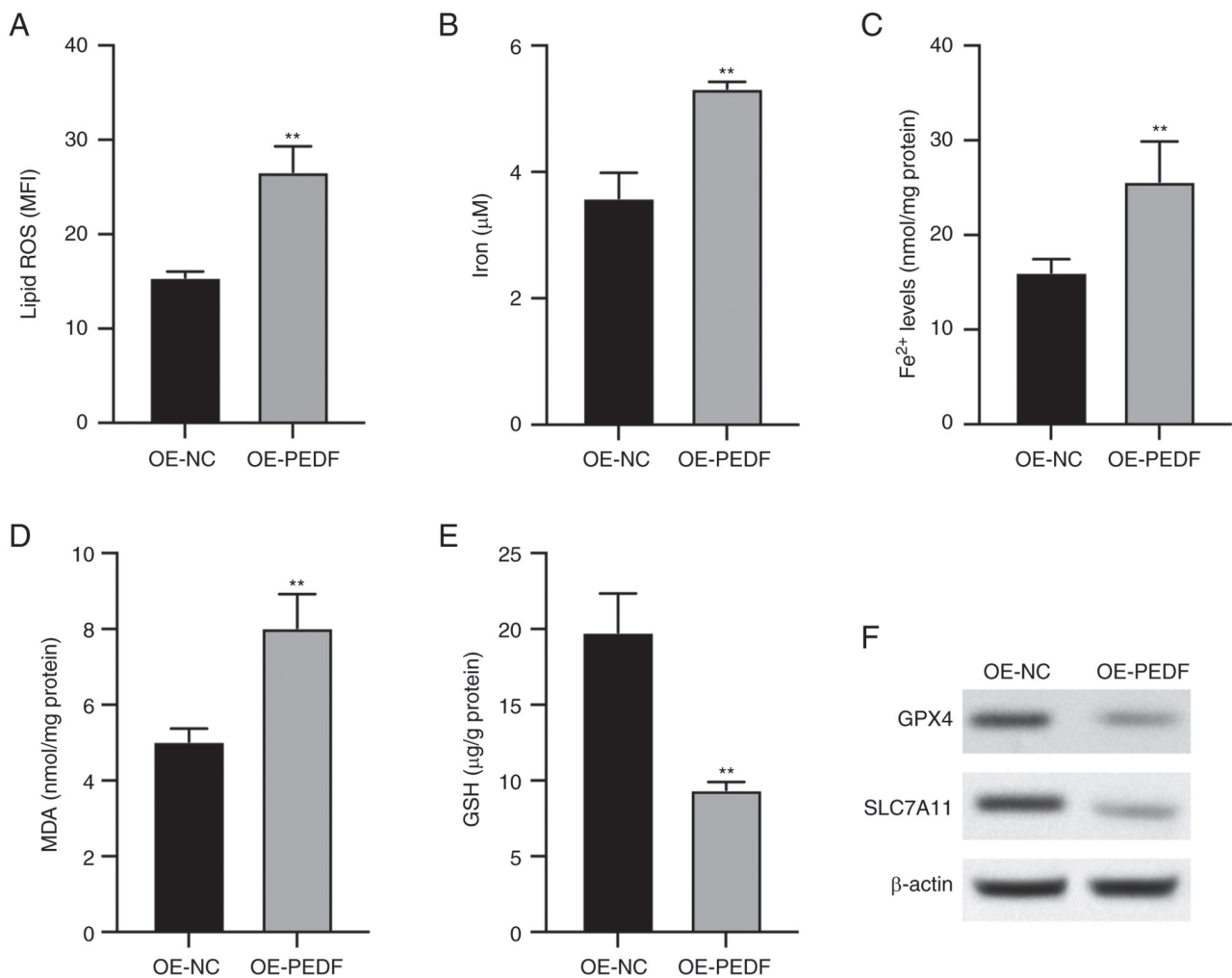


Figure 2. PEDF overexpression induces ferroptosis of extravillous trophoblast cells transfected with OE-PEDF. Levels of (A) lipid ROS, (B) total iron, (C) Fe<sup>2+</sup>, (D) MDA and (E) GSH were examined using the respective kits. (F) Protein expression levels of GPX4 and SLC7A11 determined by western blotting. Data are presented as the mean ± SD, n=3. \*\*P<0.01 vs. OE-NC. GPX4, glutathione peroxidase 4; GSH, reduced glutathione; MDA, malondialdehyde; MFI, mean fluorescence intensity; OE-NC, control empty vector for overexpression; OE-PEDF, PEDF overexpression vector; PEDF, pigment epithelium-derived factor; ROS, reactive oxygen species; SLC7A11, solute carrier family 7 member 11.

The tube formation assay was conducted to examine angiogenesis. siPEDF significantly increased the number of tubes, while PEDF overexpression significantly decreased the number of tubes compared with the siNC group or the OE-NC group, respectively (Fig. 1G). These data demonstrated that PEDF overexpression suppressed proliferation, migration and angiogenesis of EVT.

**PEDF induces ferroptosis of EVTs.** It was observed that PEDF overexpression significantly increased the levels of lipid ROS (Fig. 2A), iron (Fig. 2B), Fe<sup>2+</sup> (Fig. 2C) and MDA (Fig. 2D) compared with the control group, which are key biomarkers for ferroptosis. The levels of GSH, the antioxidant substrate of ferroptosis, were significantly decreased by PEDF overexpression (Fig. 2E), and the protein expression levels of GPX4 and SLC7A11, the ferroptosis inhibitory factors, were decreased by PEDF overexpression (Fig. 2F). These data indicated that PEDF overexpression induced ferroptosis of EVTs.

**PEDF suppresses the Wnt-β-catenin/VEGF signaling pathway in EVTs.** Subsequently, the mechanisms that participate in the

PEDF-regulated angiogenesis of EVTs were explored using a Wnt signaling activator. The overexpression of PEDF decreased the protein expression levels of Wnt and β-catenin, which were recovered by treatment with the Wnt signaling pathway agonist BML-284, with BML-284 increasing the protein expression of Wnt and β-catenin in EVTs treated with OE-PEDF (Fig. 3A). It was further observed that the relative mRNA expression levels of VEGF were significantly decreased by PEDF overexpression; however, this was reversed by BML-284 treatment, which significantly increased the relative mRNA expression levels of VEGF compared with the OE-PEDF group (Fig. 3B). The protein expression levels of VEGF were decreased by PEDF overexpression, whereas treatment with BML-284 reversed this decrease (Fig. 3C). These data indicated that PEDF suppressed Wnt signaling in EVTs.

**PEDF regulates the phenotypes of EVTs through the Wnt-β-catenin/VEGF signaling pathway.** To explore the potential mechanism of PEDF-regulated phenotypes of EVTs, the roles of the Wnt-β-catenin/VEGF signaling pathway and ferroptosis in PEDF-regulated phenotypes of EVTs were assessed by

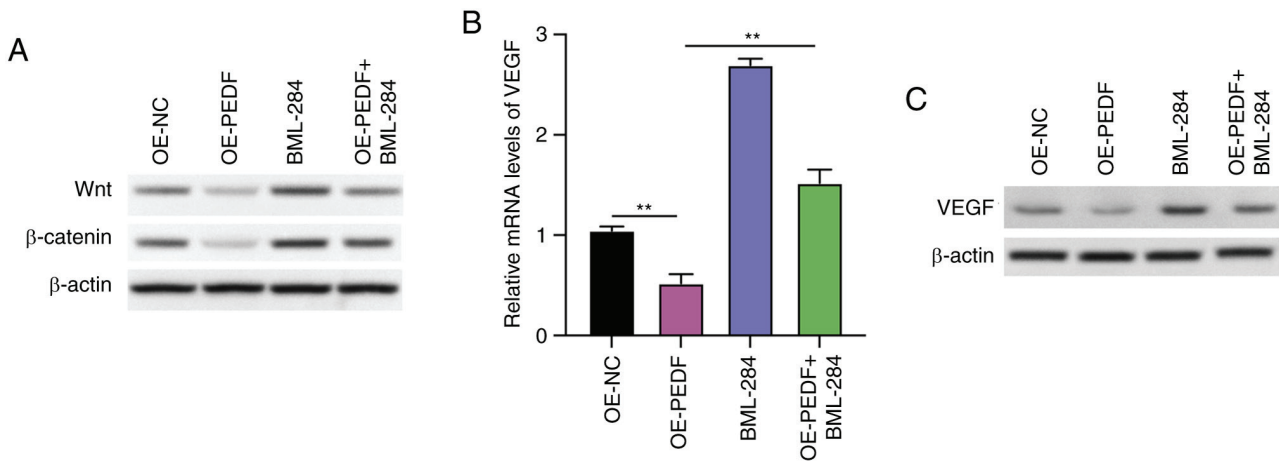


Figure 3. PEDF suppresses the Wnt- $\beta$ -catenin/VEGF signaling pathway in extravillous trophoblast cells. (A) Protein expression levels of Wnt and  $\beta$ -catenin were determined by western blotting. Relative (B) mRNA and (C) protein expression levels of VEGF were examined by reverse transcription-quantitative PCR and western blotting. Data are presented as the mean  $\pm$  SD,  $n=3$ . \*\* $P<0.01$  vs. OE-NC or OE-PEDF. OE-NC, control empty vector for overexpression; OE-PEDF, PEDF overexpression vector; PEDF, pigment epithelium-derived factor; VEGF, vascular endothelial growth factor.

treatment with the ferroptosis inhibitor Fer-1 and BML-284, and overexpression of VEGF. Inhibition of ferroptosis by Fer-1, activation of Wnt signaling by BML-284 and overexpression of VEGF increased the cell viability that was suppressed by PEDF overexpression (Fig. 4A), Edu-positive cells (Fig. 4B) and colony numbers (Fig. 4C), and enhanced the invasion (Fig. 4D), migration (Figs. 4E and S4) and angiogenesis (Fig. 4F) of EVT.

The protein expression levels of vimentin, FGF, VEGF, PDGF and PCNA were increased, and the expression levels of E-cadherin were decreased in PEDF-overexpressing EVTs treated with Fer-1 or BML-284 or transfected with OE-VEGF compared with the OE-PEDF group (Fig. 4G). These data showed that activation of the Wnt signaling pathway could reverse the suppressive effects of PEDF overexpression on the proliferation, migration and angiogenesis of EVTs, indicating that Wnt signaling and VEGF may be a mediator of PEDF-regulated EVT phenotype.

*PEDF induces ferroptosis of EVTs by suppressing the Wnt- $\beta$ -catenin/VEGF signaling pathway.* The role of the Wnt- $\beta$ -catenin/VEGF signaling pathway in PEDF-regulated ferroptosis was verified in EVTs. In PEDF-overexpressing cells, treatment with Fer-1 and BML-284 and VEGF overexpression significantly decreased the levels of lipid ROS (Fig. 5A), iron (Fig. 5B),  $Fe^{2+}$  (Fig. 5C) and MDA (Fig. 5D) compared with those in cells overexpressing PEDF. Furthermore, in PEDF-overexpressing cells, treatment with Fer-1 and BML-284, and VEGF overexpression significantly increased the GSH levels compared with those in cells overexpressing PEDF (Fig. 5E).

The PEDF-reduced levels of GPX4 and SLC7A11 were recovered by Fer-1, BML-288 and overexpression of VEGF compared with the OE-PEDF group (Fig. 5F). These data demonstrated that the Wnt- $\beta$ -catenin/VEGF signaling pathway potentially mediates PEDF-regulated ferroptosis.

## Discussion

PAS is characterized by excessive trophoblast invasion (21). According to the depth of placental invasion into the uterine

muscle layer, it can be categorized into placenta accreta, placenta increta and placenta percreta, which are dangerous complications in obstetrics (21). During normal pregnancy, after the placenta implants, mononuclear trophoblast cells begin to proliferate and form columnar cells. Some of these nourishing cells lose their proliferative ability and differentiate into cells with high invasive capabilities, similar to tumor cells, known as EVTs (2,8). EVTs exhibit a high level of invasiveness, which is a normal and controlled physiological behavior strictly regulated by the maternal body. However, various molecules, such as VEGF and Notch, can influence the invasive and angiogenic abilities of trophoblast cells, leading to early placental abnormalities, and in turn, resulting in pregnancy-related diseases associated with the placenta (22,23). PAS represents a typical example of these conditions (24,25). In patients with PAS, a significant number of EVTs are observed at the maternal-fetal interface. EVT invasion leads to changes in vascular remodeling and affects the formation of new maternal-fetal blood vessels in the uterus (24,25). Compared with a healthy placenta, patients with PAS exhibit complex and irregular blood vessel proliferation within the placenta, with tortuous vessel paths and varying diameters, indicating rich and abnormal blood flow (26). All the aforementioned findings suggest the involvement of transitional invasion by EVTs and neovascularization in PAS; however, the specific mechanisms are still not fully understood (27).

In the present study, it was demonstrated that overexpression of PEDF suppressed the proliferation, invasion and tube formation of EVTs, whereas knockdown of PEDF had the opposite effect. A decrease in the protein expression levels of PCNA, FGF, VEGF, PDGF and vimentin was observed following overexpression of PEDF, while an increase was observed following small interfering RNA knockdown of PEDF. The PCNA, FGF, VEGF and PDGF were critical regulators participate in the cell proliferation, angiogenesis and invasion; decrease of these factors following overexpression of PEDF suggested that PEDF modulated the growth and angiogenesis of EVTs.

The mechanisms underlying the altered proliferation, invasion and angiogenesis of EVTs following PEDF regulation were

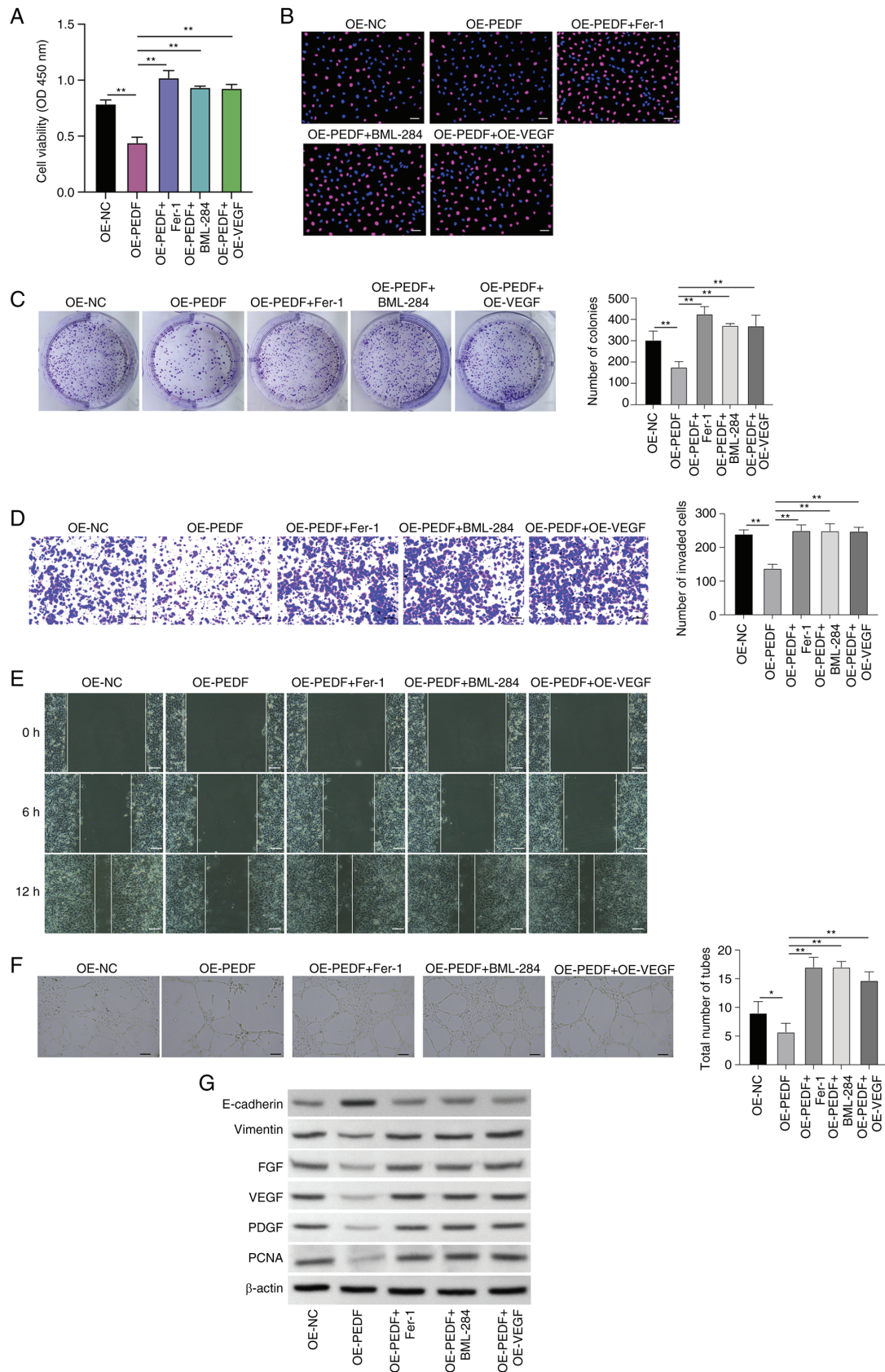


Figure 4. PEDF regulates phenotypes of EVT cells via the Wnt- $\beta$ -catenin/VEGF signaling pathway. EVT cells were transfected with OE-PEDF and treated with Fer-1 or BML-284 or transfected with OE-VEGF. Cell viability and proliferation were examined using (A) Cell Counting Kit-8, (B) 5-ethynyl-2'-deoxyuridine (red, proliferative cells; blue, nuclei) and (C) colony formation assays. Cell (D) invasion and (E) migration were assessed by Transwell and wound healing assays. (F) Angiogenesis was analyzed using a tube formation assay. (G) Expression levels of E-cadherin, vimentin, FGF, VEGF, PDGF and PCNA were examined by western blotting. Scale bar, 50  $\mu$ m. Data are presented as the mean  $\pm$  SD, n=3. \*P<0.05 and \*\*P<0.01 vs. OE-NC or OE-PEDF. EVT, extravillous trophoblast cell; Fer-1, ferrostatin-1; FGF, fibroblast growth factor; OD, optical density; OE-NC, control empty vector for overexpression; OE-PEDF, PEDF overexpression vector; OE-VEGF, VEGF overexpression vector; PCNA, proliferating cell nuclear antigen; PDGF, platelet-derived growth factor; PEDF, pigment epithelium-derived factor; VEGF, vascular endothelial growth factor.

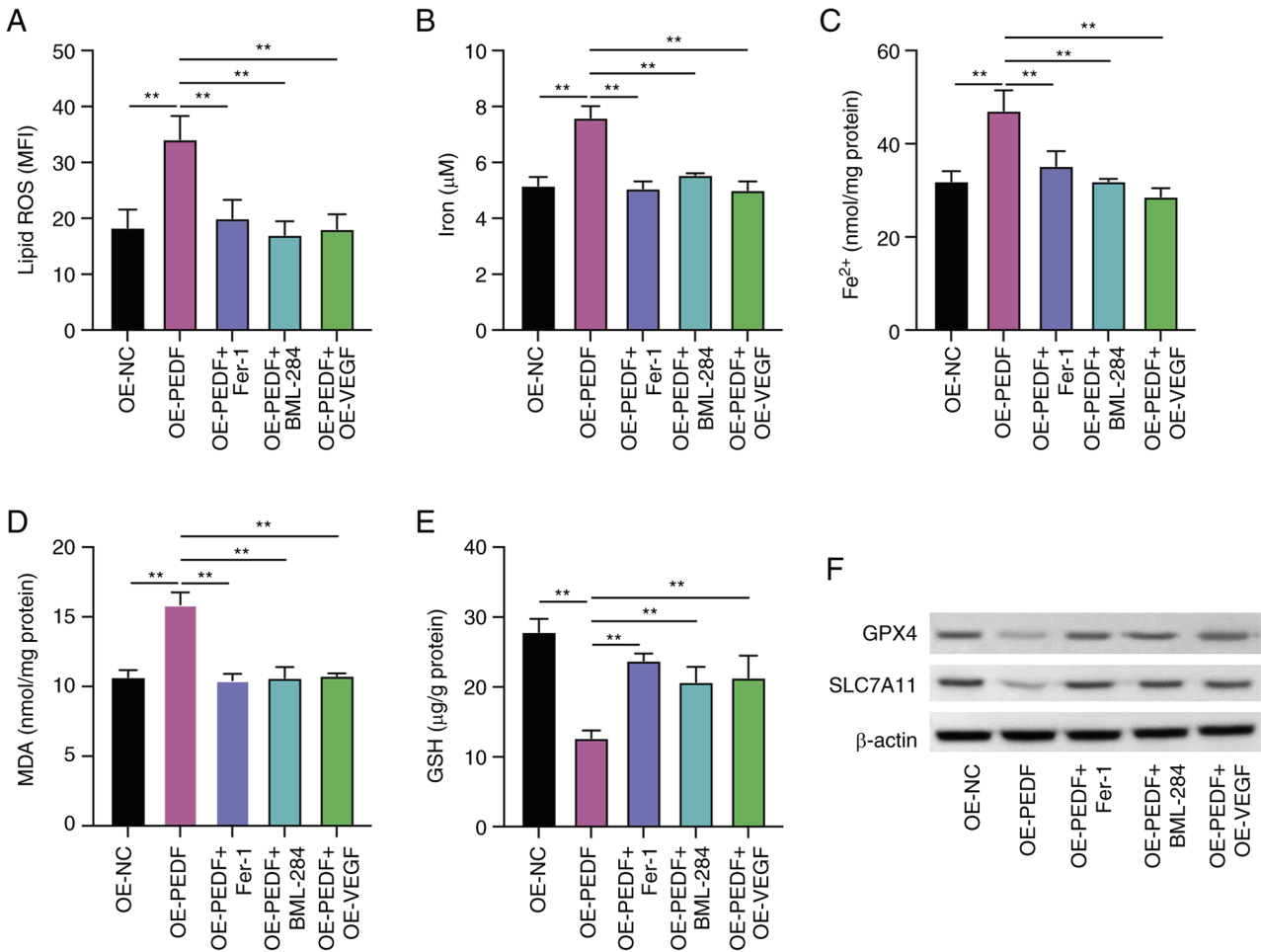


Figure 5. PEDF induces ferroptosis of EVTs by suppressing the Wnt-β-catenin/VEGF pathway. EVTs were transfected with OE-PEDF and OE-VEGF or transfected with OE-PEDF and treated with Fer-1 or BML-284. The levels of (A) lipid ROS, (B) total iron, (C) Fe<sup>2+</sup>, (D) MDA and (E) GSH were examined using the respective kits. (F) Protein expression levels of GPX4 and SLC7A11 were determined by western blotting. Data are presented as the mean ± SD, n=3. \*\*P<0.01 vs. OE-NC or OE-PEDF. EVT, extravillous trophoblast cell; Fer-1, ferostatatin-1; GPX4, glutathione peroxidase 4; GSH, reduced glutathione; MDA, malondialdehyde; MFI, mean fluorescence intensity; OE-NC, control empty vector for overexpression; OE-PEDF, PEDF overexpression vector; OE-VEGF, VEGF overexpression vector; PEDF, pigment epithelium-derived factor; ROS, reactive oxygen species; SLC7A11, solute carrier family 7 member 11; VEGF, vascular endothelial growth factor.

subsequently determined. Ferroptosis has been widely studied in recent years and is involved in various diseases (28,29). Several studies have demonstrated the participation of ferroptosis in EVT phenotypes, and that excessive iron levels can be detrimental to pregnancy (30) and is associated with reproductive disorders such as endometriosis (31). In the present study, overexpression of PEDF led to decreased proliferation of HTR-8/SVneo cells, along with the induction of ferroptosis, which was detected by the accumulation of lipid ROS, increases in total iron, Fe<sup>2+</sup> and MDA levels, and the decreased levels of GSH, as well as decreased protein expression levels of GPX4 and SLC7A11, which are inhibitors of ferroptosis. The detection of total iron and Fe<sup>2+</sup> levels was a specific indication of ferroptosis induction and should be sufficient to rule out the possibility of the results arising from oxidative damage, pyroptosis or other mechanisms (32). These data indicated that PEDF may contribute to ferroptosis of EVTs.

In a previous study, the relative expression levels of PEDF and VEGF in placenta from healthy and PAS clinical samples were analyzed (33). It was identified that in the group with abnormal placental positions (placenta accreta and placenta

previa), there was a low level of PEDF in the placenta. This low expression was negatively associated with the VEGF level and microvessel density, which suggests that the reduced expression of PEDF in the placental tissue of the group with abnormal placental positions may contribute to insufficient negative regulation of VEGF and the pathological vascular formation in the placenta (34). However, the detailed molecular mechanisms by which PEDF regulates PAS are unclear.

Furthermore, in the present study, it was demonstrated that the protein expression levels of Wnt, β-catenin and VEGF were decreased following overexpression of PEDF, which is consistent with a previous study demonstrating that PEDF can suppress Wnt signaling (35). The PEDF-suppressed proliferation and angiogenesis of EVTs were recovered by treatment with the Wnt agonist BML-284, suggesting that PEDF regulated VEGF expression and EVT phenotypes via the Wnt/β-catenin signaling pathway.

Furthermore, the Wnt signaling pathway serves a critical role in cell differentiation, and stemness maintenance during the development of tissues and organs (36,37). When the pathway is activated, the Wnt receptors prevent the degradation

of  $\beta$ -catenin, which consequently stimulates the function of transcription factors T-cell factor/lymphoid enhancer factor and the expression of targeted genes, including VEGF (38). Wnt is necessary for the expansion of trophoblast progenitors and stem cells (7). It has been reported that Wnt-3a activation induces matrix metalloproteinase-2 secretion and trophoblast migration (5). In the present study, it was demonstrated that the VEGF protein expression and tube formation of EVT were suppressed by PEDF overexpression and were recovered by Wnt pathway activation by treatment with BML-284. Therefore, it was predicted that PEDF modulated Wnt signaling to suppress VEGF expression and angiogenesis.

To summarize, it was determined that PEDF overexpression inhibited the proliferation, invasion and angiogenesis of EVTs, and induced ferroptosis by modulating Wnt signaling to suppress VEGF expression. The present study revealed the importance of ferroptosis in PEDF-regulated EVT functions and provided novel evidence for the pathological role of PEDF in PAS.

### Acknowledgements

This abstract was presented at the Chinese Medical Association 17<sup>th</sup> National Conference on Perinatal Medicine (November 17-19, 2023; Guangzhou, China), and was published as Abstract no. PO-295.

### Funding

This study was supported by Fujian Province Health and Health Science and Technology Program Projects (grant no. 2020GGB006).

### Availability of data and materials

The data generated in the present study may be requested from the corresponding author.

### Authors' contributions

LZ designed the study. RL and LZ wrote the manuscript. RL, XW, XH and JW performed the experiments. RL and XW performed statistical analysis of the data. LZ, RL, XW, XH and JW confirm the authenticity of all raw data. All authors read and approved the final manuscript.

### Ethics approval and consent to participate

All experiments concerning clinical samples were approved by the Ethics Committee of Shengli Clinical Medical College of Fujian Medical University (approval no. K2020-090040; Fuzhou, China). All patients provided written informed consent for participation.

### Patient consent for publication

Not applicable.

### Competing interests

The authors declare that they have no competing interests.

### References

- Moser G and Huppertz B: Implantation and extravillous trophoblast invasion: From rare archival specimens to modern biobanking. *Placenta* 56: 19-26, 2017.
- Wei XW, Zhang YC, Wu F, Tian FJ and Lin Y: The role of extravillous trophoblasts and uterine NK cells in vascular remodeling during pregnancy. *Front Immunol* 13: 951482, 2022.
- Illsley NP, DaSilva-Arnold SC, Zamudio S, Alvarez M and Al-Khan A: Trophoblast invasion: Lessons from abnormally invasive placenta (placenta accreta). *Placenta* 102: 61-66, 2020.
- Horgan R and Abuhamad A: Placenta accreta spectrum: Prenatal diagnosis and management. *Obstet Gynecol Clin North Am* 49: 423-438, 2022.
- Sonderegger S, Haslinger P, Sabri A, Leisser C, Otten JV, Fiala C and Knöfler M: Wingless (Wnt)-3A induces trophoblast migration and matrix metalloproteinase-2 secretion through canonical Wnt signaling and protein kinase B/AKT activation. *Endocrinology* 151: 211-220, 2010.
- Knöfler M and Pollheimer J: Human placental trophoblast invasion and differentiation: A particular focus on Wnt signaling. *Front Genet* 4: 190, 2013.
- Dietrich B, Haider S, Meinhardt G, Pollheimer J and Knöfler M: WNT and NOTCH signaling in human trophoblast development and differentiation. *Cell Mol Life Sci* 79: 292, 2022.
- Pollheimer J, Vondra S, Baltayeva J, Beristain AG and Knöfler M: Regulation of placental extravillous trophoblasts by the maternal uterine environment. *Front Immunol* 9: 2597, 2018.
- Abbas Y, Turco MY, Burton GJ and Moffett A: Investigation of human trophoblast invasion in vitro. *Hum Reprod Update* 26: 501-513, 2020.
- Shang Z, Li C, Liu X, Xu M, Zhang X, Li X, Barnstable CJ, Zhao S and Tombran-Tink J: PEDF gene deletion disrupts corneal innervation and ocular surface function. *Invest Ophthalmol Vis Sci* 62: 18, 2021.
- Ma B, Zhou Y, Liu R, Zhang K, Yang T, Hu C, Gao Y, Lan Q, Liu Y, Yang X and Qi H: Pigment epithelium-derived factor (PEDF) plays anti-inflammatory roles in the pathogenesis of dry eye disease. *Ocul Surf* 20: 70-85, 2021.
- Ansari D, Althini C, Ohlsson H, Bauden M and Andersson R: The role of PEDF in pancreatic cancer. *Anticancer Res* 39: 3311-3315, 2019.
- Bao X, Zeng J, Huang H, Ma C, Wang L, Wang F, Liao X and Song X: Cancer-targeted PEDF-DNA therapy for metastatic colorectal cancer. *Int J Pharm* 576: 118999, 2020.
- Loegl J, Nussbaumer E, Hiden U, Majali-Martinez A, Ghaffari-Tabrizi-Wizy N, Cvitic S, Lang I, Desoye G and Huppertz B: Pigment epithelium-derived factor (PEDF): A novel trophoblast-derived factor limiting fetoplacental angiogenesis in late pregnancy. *Angiogenesis* 19: 373-388, 2016.
- Li J, Cao F, Yin HL, Huang ZJ, Lin ZT, Mao N, Sun B and Wang G: Ferroptosis: Past, present and future. *Cell Death Dis* 11: 88, 2020.
- Wei X, Yi X, Zhu XH and Jiang DS: Posttranslational modifications in ferroptosis. *Oxid Med Cell Longev* 2020: 8832043, 2020.
- Wu X, Li Y, Zhang S and Zhou X: Ferroptosis as a novel therapeutic target for cardiovascular disease. *Theranostics* 11: 3052-3059, 2021.
- Chen X, Kang R, Kroemer G and Tang D: Ferroptosis in infection, inflammation immunity. *J Exp Med* 218: e20210518, 2021.
- Hirschhorn T and Stockwell BR: The development of the concept of ferroptosis. *Free Radic Biol Med* 133: 130-143, 2019.
- Livak KJ and Schmittgen TD: Analysis of relative gene expression data using real-time quantitative PCR and the 2(-Delta Delta C(T)) method. *Methods* 25: 402-408, 2001.
- Bloomfield V, Rogers S and Leyland N: Placenta accreta spectrum. *CMAJ* 192: E980, 2020.
- Zhang Q, Yu S, Huang X, Tan Y, Zhu C, Wang YL, Wang H, Lin HY, Fu J and Wang H: New insights into the function of Cullin 3 in trophoblast invasion and migration. *Reproduction* 150: 139-149, 2015.
- Scalise ML, Amaral MM, Reppetti J, Damiano AE, Ibarra C and Sacerdoti F: Cytotoxic effects of Shiga toxin-2 on human extravillous trophoblast cell lines. *Reproduction* 157: 297-304, 2019.
- Jauniaux E, Jurkovic D, Hussein AM and Burton GJ: New insights into the etiopathology of placenta accreta spectrum. *Am J Obstet Gynecol* 227: 384-391, 2022.
- Ma Y, Hu Y and Ma J: Animal models of the placenta accreta spectrum: Current status and further perspectives. *Front Endocrinol (Lausanne)* 14: 1118168, 2023.

26. Xia H, Ke SC, Qian RR, Lin JG, Li Y and Zhang X: Comparison between abdominal ultrasound and nuclear magnetic resonance imaging detection of placenta accreta in the second and third trimester of pregnancy. *Medicine (Baltimore)* 99: e17908, 2020.
27. Burton GJ and Jauniaux E: Pathophysiology of placental-derived fetal growth restriction. *Am J Obstet Gynecol* 218: S745-S761, 2018.
28. Sun Y, Chen P, Zhai B, Zhang M, Xiang Y, Fang J, Xu S, Gao Y, Chen X, Sui X and Li G: The emerging role of ferroptosis in inflammation. *Biomed Pharmacother* 127: 110108, 2020.
29. Pan Q, Luo Y, Xia Q and He K: Ferroptosis and liver fibrosis. *Int J Med Sci* 18: 3361-3366, 2021.
30. Georgieff MK, Krebs NF and Cusick SE: The benefits and risks of iron supplementation in pregnancy and childhood. *Annu Rev Nutr* 39: 121-146, 2019.
31. Li Y, Zeng X, Lu D, Yin M, Shan M and Gao Y: Erastin induces ferroptosis via ferroportin-mediated iron accumulation in endometriosis. *Hum Reprod* 36: 951-964, 2021.
32. Tang D, Chen X, Kang R and Kroemer G: Ferroptosis: Molecular mechanisms and health implications. *Cell Res* 31: 107-125, 2021.
33. Ortega MA, Saez MÁ, Asúnsolo Á, Romero B, Bravo C, Coca S, Sainz F, Álvarez-Mon M, Buján J and García-Honduvilla N: Upregulation of VEGF and PEDF in placentas of women with lower extremity venous insufficiency during pregnancy and its implication in villous calcification. *Biomed Res Int* 2019: 5320902, 2019.
34. Duzyj CM, Buhimschi IA, Laky CA, Cozzini G, Zhao G, Wehrum M and Buhimschi CS: Extravillous trophoblast invasion in placenta accreta is associated with differential local expression of angiogenic and growth factors: A cross-sectional study. *BJOG* 125: 1441-1448, 2018.
35. Protiva P, Gong J, Sreekumar B, Torres R, Zhang X, Belinsky GS, Cornwell M, Crawford SE, Iwakiri Y and Chung C: Pigment epithelium-derived factor (PEDF) inhibits Wnt/ $\beta$ -catenin signaling in the liver. *Cell Mol Gastroenterol Hepatol* 1: 535-549, e14, 2015.
36. Li Y, Baccouche B, Olayinka O, Serikbaeva A and Kazlauskas A: The role of the Wnt pathway in VEGF/anti-VEGF-dependent control of the endothelial cell barrier. *Invest Ophthalmol Vis Sci* 62: 17, 2021.
37. Jiang L, Yin M, Wei X, Liu J, Wang X, Niu C, Kang X, Xu J, Zhou Z, Sun S, *et al*: Bach1 represses Wnt/ $\beta$ -catenin signaling and angiogenesis. *Circ Res* 117: 364-375, 2015.
38. Kovács B, Vajda E and Nagy EE: Regulatory effects and interactions of the Wnt and OPG-RANKL-RANK signaling at the bone-cartilage interface in osteoarthritis. *Int J Mol Sci* 20: 4653, 2019.



Copyright © 2024 Li *et al*. This work is licensed under a Creative Commons Attribution-NonCommercial-NoDerivatives 4.0 International (CC BY-NC-ND 4.0) License.